CellPress

Molecular Cell

Technology review

Next generation single-molecule techniques: Imaging, labeling, and manipulation *in vitro* and *in cellulo*

Taekjip Ha,[1,2,3,4,*] Christian Kaiser,[5] Sua Myong,[2] Bin Wu,[1] and Jie Xiao[1]
[1]Department of Biophysics and Biophysical Chemistry, Johns Hopkins School of Medicine, Baltimore, MD 21205, USA
[2]Department of Biophysics, Johns Hopkins University, Baltimore, MD 21218, USA
[3]Department of Biomedical Engineering, Johns Hopkins University, Baltimore, MD 21218, USA
[4]Howard Hughes Medical Institute, Baltimore, MD 21205, USA
[5]Department of Biology, Johns Hopkins University, Baltimore, MD 21218, USA
*Correspondence: tjha@jhu.edu
https://doi.org/10.1016/j.molcel.2021.12.019

SUMMARY

Owing to their unique abilities to manipulate, label, and image individual molecules *in vitro* and *in cellulo*, single-molecule techniques provide previously unattainable access to elementary biological processes. In imaging, single-molecule fluorescence resonance energy transfer (smFRET) and protein-induced fluorescence enhancement *in vitro* can report on conformational changes and molecular interactions, single-molecule pull-down (SiM-Pull) can capture and analyze the composition and function of native protein complexes, and single-molecule tracking (SMT) in live cells reveals cellular structures and dynamics. In labeling, the abilities to specifically label genomic loci, mRNA, and nascent polypeptides in cells have uncovered chromosome organization and dynamics, transcription and translation dynamics, and gene expression regulation. In manipulation, optical tweezers, integration of single-molecule fluorescence with force measurements, and single-molecule force probes in live cells have transformed our mechanistic understanding of diverse biological processes, ranging from protein folding, nucleic acids-protein interactions to cell surface receptor function.

INTRODUCTION

The past two decades have witnessed the emergence of powerful biotechnologies from various disciplines. In particular, single-molecule technologies, with their unique abilities to image, label, and manipulate individual biomolecules provide previously unattainable access to elementary biological processes, thus revolutionizing biological inquiries.

The major technological themes of this review include (1) single-molecule imaging *in vitro*, in-cell lysate and live cells at high resolution, sensitivity, throughput, and biocompatibility; (2) in-cell single-molecule labeling of genomic DNA loci, mRNA transcripts and nascent polypeptides, permitting direct measurements of transcription and translation dynamics; and (3) single-molecule manipulation using optical tweezers and its integration with single-molecule fluorescence imaging, and single-molecule tension sensors. By matching the length and timescales of biological processes under native or close to native conditions, these technologies enable the interrogation of the organization and dynamics of nanoscale machineries well beyond the traditional limit, providing a window into the actual operation of cells.

SINGLE-MOLECULE IMAGING

smFRET and smPIFE

The imaging of single fluorophores tells us that the labeled biological molecule is present, for example, binding of ATP to a motor protein and its dissociation after hydrolysis, where the molecule is during its directional or diffusive movements, the composition of a protein complex, and conformational changes and protein assembly dynamics during function.

Many biomolecular processes, including protein-nucleic acid interactions and conformational changes within proteins, occur through inter- and intra-molecular rearrangements of specific interactions. High-resolution structural analyses provide snapshots of these processes in atomic detail but are typically blind to the time evolution of these dynamic interactions or conformational transitions. Conventional biochemical methods including surface plasmon resonance, isothermal titration calorimetry, electrophoretic mobility shift assays, fluorescence spectroscopy, anisotropy and stopped-flow capture ensemble behavior of molecule populations, yet, often miss molecular heterogeneity and require the synchronization of the reaction. Single-molecule imaging overcomes these drawbacks and enables the observation of individual molecules undergoing dynamic motions.

Among the many implementations of single-molecule fluorescence imaging *in vitro*, single-molecule fluorescence resonance energy transfer (smFRET) between a donor and an acceptor fluorophore (Figure 1A), is one of the most powerful and popular methods due to its strong dependence on molecular-scale distances (~0.5 to 10 nm). Since its initial demonstration (Ha et al., 1996), smFRET has been extended to three or more colors (Hohng et al., 2004) to record multiple reaction coordinates simultaneously and combined with optical tweezers to measure

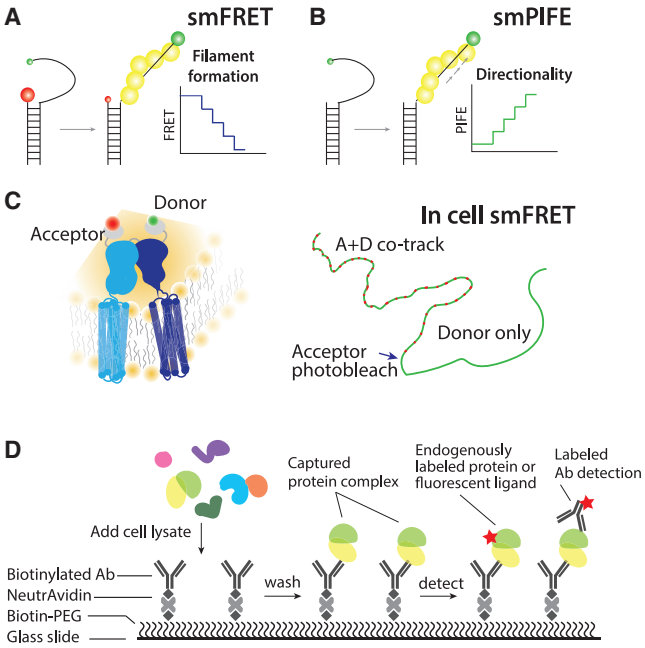

Figure 1. Illumstration of smFRET, smPIFE, and SiMPull

(A) When a protein filament assembles on a single-stranded DNA separating the donor (green) and the acceptor fluorophore (red) one monomer at a time, a stepwise decrease in FRET is observed over time due to DNA stretching.

(B) smPIFE shows a stepwise signal increase when the protein filament grows toward the donor-labeled DNA end via monomer by monomer addition.

(C) f smFRET in live cells to monitor the dimer of a G-protein-coupled receptor and its diffusional movement on cell membrane through co-tracking. Acceptor photobleaching results in donor signal increase, confirming the presence of FRET.

(D) Schematics of SiMPull. A biotinylated antibody on a passivated surface captures a protein complex of interest from cell extracts. After washing away unbound cell extracts, the captured complex is detected via single-molecule fluorescence imaging either using fluorescently labeled antibodies or fluorescent reporter fusion.

even minute conformational dynamics as a function of force (Hohng et al., 2007). Most commonly, total internal reflection fluorescence (TIRF) microscopy of surface-immobilized molecules is used for smFRET measurements. Alternatively, solution-based detection under alternating laser excitation can be performed to sort molecules based on donor and acceptor stoichiometry and measure smFRET efficiencies without surface tethering (Kapanidis et al., 2004), but suffers from limited photon counts due to a short observation duration of molecules diffusing through the focused excitation laser beam. The anti-Brownian electrokinetic (ABEL) trap enables extremely long observation windows by canceling out the Brownian motion of a molecule through electrophoretic drift via feedback, limited only by photobleaching, hence dramatically increasing photon counts and consequently precision (Wilson and Wang, 2021). However, the ABEL trap follows only one molecule at a time, it has a much lower throughput than TIRF-based detection, which can simultaneously image hundreds of individual molecules in a field of view.

Single-molecule protein-induced fluorescence enhancement (smPIFE) is a simple yet powerful technique for following dynamic protein-nucleic acid interactions without having to fluorescently label the protein (Hwang et al., 2011) (Figure 1B). In smPIFE, a single fluorophore conjugated to DNA or RNA reports on the binding and dissociation of interacting molecules: the fluorescence signal increases upon protein binding in the proximity, hence the name. Fluorophores such as Cy3 exist as *cis*- and *trans*-isomers, which represent photo-inactive (due to rapid non-radiative decay) and photo-active states, respectively. The *trans* isomer is selectively stabilized by protein binding, hence increasing the fluorescence lifetime and quantum yield, resulting in fluorescence enhancement. The distance sensitivity of FRET (3–8 nm) is nicely complemented by that of PIFE (0–4 nm). Therefore, the two techniques, when strategically deployed, produce complementary information. One example is the Rad51 filament formation in which smFRET revealed a stepwise assembly of the Rad51 filament (Figure 1A), whereas smPIFE clarified the direction of filament growth (Figure 1B) (Qiu et al., 2013). A potential complication of smFRET interpretation is that quantum yield changes in the fluorophores due to PIFE can cause changes in FRET even when there is no actual distance change. Therefore, a generalizable procedure to characterize and decouple the PIFE contribution from FRET experiments in various protein and nucleic acid systems needs to be developed. A recent team effort, involving numerous investigators, has called for establishing standard practices of conducting experiments, analyzing results, and deducing information from these single-molecule detection platforms (Lerner et al., 2021).

One exciting new application of smFRET is the imaging and tracking of transmembrane receptors, as was recently demonstrated for G-protein coupled receptor (GPCR) dimers in live mammalian cells (Asher et al., 2021). Taking advantage of the self-labeling and self-healing tags to site-specifically label GPCR proteins, the authors directly probed their homo- versus heterodimer state by tracking the smFRET signal of individual receptors (Figure 1C). It is also becoming possible to apply the approach to soluble proteins in cells (König et al., 2015), which will be a powerful tool for resolving dynamic stoichiometries of a wide variety of macromolecular complexes. While versatile, smFRET and smPIFE are limited to a narrow distance range. DNA curtains provide a means of probing long-distance search processes and translocation movement of DNA-binding protein complexes such as CRISPR-Cas systems at the single-molecule level with high throughput (Redding et al., 2015).

SiMPull

Protein-protein interaction and protein complex formation has traditionally been studied by biochemical methods such as pull-down or co-immunoprecipitation assays. However, these methods do not provide accurate compositional information when one protein is present in multiple and distinct complexes. It is also difficult to determine the number of copies of each component in a protein complex, and lengthy biochemical purification procedures could lead to loss or alteration of physiological complexes. Single-molecule pull-down (SiMPull) (Jain et al., 2011) combines principles of conventional immuno-pull-down assays and TIRF microscopy to enable direct visualization of cellular protein complexes at the single-molecule level (Figure 1D). When cell extracts are added to a passivated imaging surface coated with antibodies against the protein of interest, the surface-tethered antibody captures the target protein

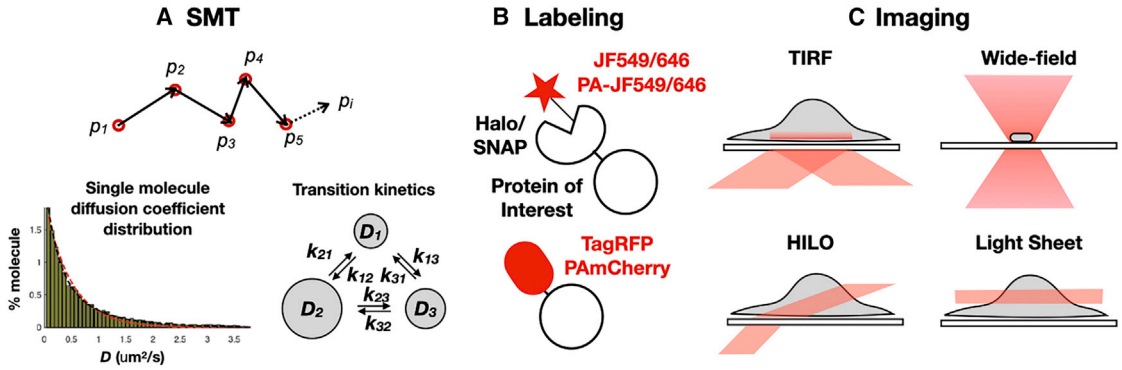

Figure 2. Illustration of single-molecule tracking principles, labeling, and imaging strategies

(A) Top: a schematic drawing of a SMT trajectory with multiple positions (p_{1-i}) tracked along the time. Bottom left: a representative histogram of the apparent diffusion coefficients of single molecules obtained from a SMT experiment of a DNA-binding protein shows a large spread. Bottom right: from long SMT trajectories the transition kinetics from different diffusive states can be obtained.

(B) Currently best-performing organic (JF dyes, top) and FPs (bottom) for SMT.

(C) Four commonly used microscopy illumination modes for SMT.

together with any interacting partners. After washing away unbound cell extract, associated proteins are visualized either through immunofluorescence labeling or by using genetically encoded fluorescent protein fusion tags. Different subcomplex formations can be distinguished using multi-color detection and colocalization. Furthermore, when proteins are fluorescently labeled, photobleaching events can yield information on stoichiometry, which has revealed novel stoichiometric information, for example, on auxiliary subunits of ion channels (Ávalos Prado et al., 2021; Yu et al., 2021), and transcriptional regulators (Park et al., 2020). Judicious site-specific protein labeling with unnatural amino acids has been used to perform smFRET on SiMPulled glutamate receptors to reveal activation-induced conformational rearrangements (Liauw et al., 2021). A recent method for flat field illumination avoids uneven excitation intensity across the field of view and promises to deliver stoichiometry information without the photobleaching analysis by using only the intensity information (Khaw et al., 2018). A deep learning-based approach may also be used to automate stoichiometry analysis from single-molecule intensity traces (Xu et al., 2019).

A less explored advantage of SiMPull over conventional pull-down is that the sample requirement is minuscule. Compared with western blots, which require material from more than 5,000 cells, SiMPull can detect highly expressed proteins from as few as 10 cells (Jain et al., 2011). Recently, approaches for capturing proteins from single cells have been demonstrated for bacterial cells (Wang et al., 2018b) and *C. elegans* embryos (Dickinson et al., 2017), and SiMPull was used to analyze the composition of the PAR complex during embryo polarization (Dickinson et al., 2017). Pushing the technology to the clinical realm, it has become possible to directly capture and analyze trace amounts of proteins from human blood samples, as was demonstrated for membrane and intracellular antigens using miniature fluid handling to avoid dilution and oscillatory flow-facilitated sample loading to increase protein capture yield (Mao et al., 2021). With the advent of cryoelectron microscopy (cryoEM) structural determination of native protein complexes directly captured from native animal tissues, as was shown for AMPA receptor complexes from mouse hippocampus, we can now perform SiMPull in parallel with atomic resolution structural analysis (Yu et al., 2021). It is conceivable that a similar approach may yield, in the near future, correlative cryoEM single particle reconstruction and SiMPull analysis of protein complexes isolated from human patient tissues.

SMT

Single-molecule tracking (SMT) probes the motion of single molecules in live cells. From SMT trajectories (spatial coordinates versus time) one can identify not only the molecule's diffusive movement but also its population heterogeneity and switching kinetics between different diffusive modes (Elf and Barkefors, 2019) (Figure 2A). As such, this technique offers an invaluable window to examine the molecule's dynamic interactions in real-time within the native cellular environment (Bohrer and Xiao, 2020).

High localization precision and long single-molecule recordings are key for defining the mode of movement of the molecular and for detecting its changing interactions with binding partners and/or the cellular surroundings. Currently, the best-performing SMT fluorophores are Janelia Fluor (JF) 549 and 646 (Lavis, 2017) (Figure 2B). They are bright, membrane-permeable, and red-shifted organic fluorophores that can be conjugated with a Halo or SNAP ligand to label covalently a Halo- or SNAP-tagged proteins of interest, yielding a localization precision of 20–40 nm in live cells. Their unique, rigid fluorophore structure also ensures low photobleaching and high quantum yields, enabling the collection of long trajectories in the range of a few hundred frames under appropriate imaging conditions. If an organic fluorophore is not an option, TagRFP-T is a fluorescent protein alternative with exceptional stability (Yang et al., 2021).

Another class of fluorophores, photo-convertible FPs such as PAmCherry and organic fluorophores PA-JF549/646 (Grimm et al., 2016), become fluorescent only upon photoactivation. This property makes it possible to image the same imaging area continuously until all labeled fluorophores are activated and bleached, dramatically increasing the data throughput. Their

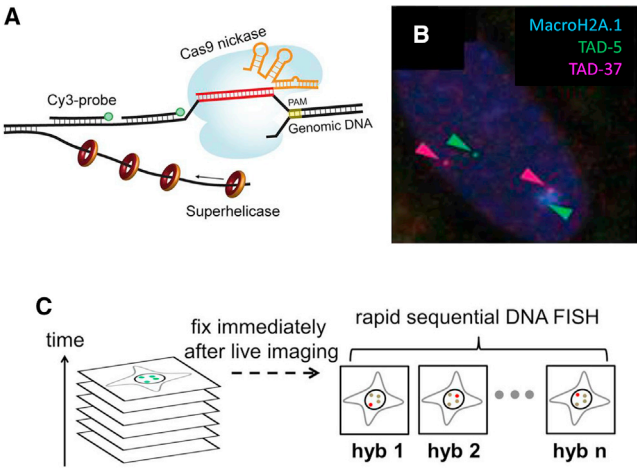

Figure 3. Illustration of genome imaging technologies

(A) GOLD FISH schematics. Cas9 nickase creates a nick that is used to load a super helicase that unwinds DNA downstream to expose the binding sites for fluorescently labeled oligonucleotide probes.

(B) GOLD FISH image of two topologically associated domains (TADs) in chromosome X. Immunofluorescence of MacroH2A.1 marks inactive chromosome X. Source: Wang et al. (2021b).

(C) Schematics of live imaging followed by multiplexed FISH. Live imaging of fluorescent proteins does not tell us where in the genomic DNA the proteins are bound but a subsequent cell fixation and high throughput DNA FISH can reveal the location of genomic regions of interest. Source: Guan et al. (2017).

photostability and brightness, however, need to be further improved to match their non-activatable counterparts.

SMT is typically limited to detecting molecules that diffuse slowly (diffusion constant <5 $\mu m^2/s$). Stronger laser power and faster acquisition enabled by the recent development of solid-state lasers and scientific CMOS (complementary metal-oxide-semiconductor) cameras partially alleviate this limit, but high excitation intensity leads to rapid photobleaching. Thus, SMT is most commonly applied to track proteins in membranes, in the nucleus, and crowded subcellular environments. The use of nanoparticles bypasses the photobleaching problem, but their suboptimal biocompatibility requires further improvement.

TIRF microscopy is most commonly used for SMT (Figure 2C) since it reduces cellular background fluorescence, thus making it particularly suitable for membrane proteins. Other setups, including wide-field microscopy for small bacterial cells, and highly inclined and laminated optical sheet (HILO) microscopy (Tokunaga et al., 2008) and light-sheet microscopy (Gebhardt et al., 2013) for eukaryotic cytoplasmic and nucleus proteins, are also common. Analysis of SMT trajectories can be complicated and often depends on the particular needs of a given experiment. Nevertheless, the use of the ImageJ plugin Thunderstorm to localize and link single fluorescent spots (Ovesný et al., 2014), followed by a hidden Markov model analysis to extract transition kinetics (Persson et al., 2013) has been implemented successfully.

Recently, new developments in hardware engineering and tracking algorithms made it possible to track fast diffusing molecules (up to 10 $\mu m^2/s$) with a high frame rate (~10 kHz) and in three dimensions (Hou et al., 2020) (Schmidt et al., 2021). Two or three-color SMT to analyze protein interaction and complex formation have also been demonstrated (Sungkaworn et al., 2017) (Chen et al., 2021). These new emerging technologies will continue to expand the types of biological problems that can be attacked by SMT.

SINGLE-MOLECULE LABELING

Labeling is a prerequisite for sensitive, specific, and accurate single-molecule detection, but it is challenging to develop a strategy that faithfully reports biological processes without perturbing them and without labeling irrelevant molecules nonspecifically.

Genome labeling

The three-dimensional organization of the genome regulates gene expression and DNA-related processes. Chromosome conformation capture and its derivatives are most commonly used to identify sequence-specific genomic interactions, but they cannot provide spatial information of where interactions take place. Super-resolution imaging of global DNA-binding proteins (DBP) can illustrate the overall spatial organization of the genome but it is unable to match specific DNA sequences with its spatial localization. Fluorescence *in situ* hybridization (FISH) uses a set of dye-labeled short oligonucleotides to hybridize with DNA so that selected genomic loci can be imaged in single cells. DNA FISH combined with barcoding-based multiplexing and super-resolution imaging has been used to trace targeted chromosomes in single cells and to map their conformations in high resolution (Bintu et al., 2018).

Traditional DNA FISH, however, requires heat denaturation, which disrupts fine structural details of chromatin below 1 Mb. Three approaches have been developed to bypass heat denaturation. resolution after single-strand exonuclease resection (RASER) FISH uses ultraviolet light to randomly generate nicks and exonucleases to digest from the nicks to expose binding sites for FISH Probes (Brown et al., 2018). As RASER FISH still exposes the genome globally, probes can bind nonspecifically to other regions of the genome of a similar sequence. CASFISH decorates genomic regions of interest using catalytically dead Cas9 (dCas9) with a fluorescent label, therefore does not require genome denaturing (Deng et al., 2015). However, because stable binding of Cas9 to DNA requires only a ~10 bp match between its guide RNA and the target strand, there is substantial background due to nonspecific binding, making it impractical to label non-repetitive sequences. Genome oligopaint via local denaturation (GOLD) FISH overcomes the limitations of RASER FISH by locally denaturing only a region of interest, and CASFISH by relying on more specific nuclease activity of Cas9 (16 bp) than binding. In GOLD FISH (Wang et al., 2021b), genomic DNA is locally denatured by the programed loading of a super helicase Rep-X (Arslan et al., 2015) at nicks generated by the Cas9 nickase (Figures 3A and 3B). A major limitation of GOLD FISH, shared by all FISH technologies, is that it only provides a static snapshot and cannot be used to probe genomic dynamics in living cells.

For live imaging of genomic sites, dCas9 binding to endogenous loci and DBP targeted to exogenously integrated binding sites are the two most common approaches. Both generally require repetitive sequences as the target, with some exceptions, because singly labeled dCas9 or DBP are difficult to detect due to the high background of free labeled proteins and

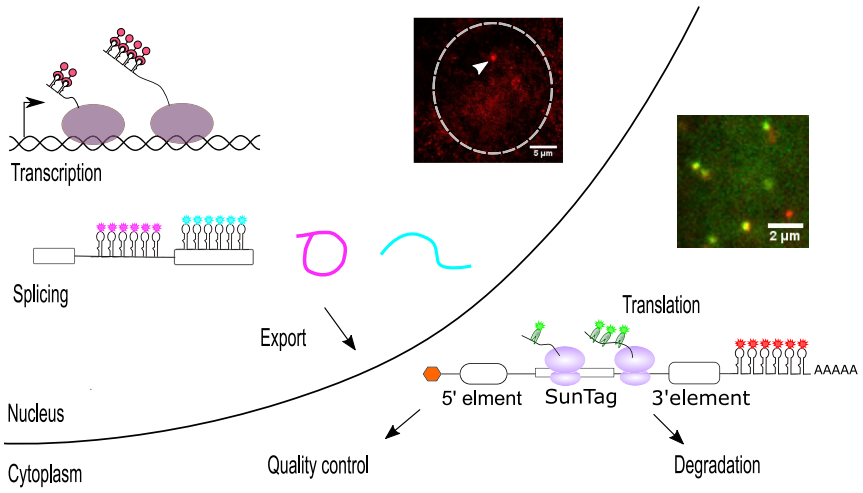

Figure 4. Visualization of nascent RNA and proteins allows measurement transcription, splicing, transport, and translation dynamics

By labeling introns and exons with two different stem-loops, kinetic competition between co-transcriptional and post-transcriptional splicing pathways can be analyzed (Coulon et al., 2014). Integration of MS2 in introns of hundreds of endogenous genes (Wan et al., 2021) showed that all these genes are transcribed in bursts. Interestingly, the splicing of introns shows vast kinetic variations, which are inconsistent with a single deterministic splicing event, but instead can be explained by a stochastic recursive-splicing model.

autofluorescence in the nucleus. The dCas9-based approach is more general as it can target any repetitive elements in the genome but is incompatible with applications that require catalytically active Cas9. Most recently, truncated guide RNA with Cas9 was used to label a repetitive region without cleaving it while a full-length guide targeting a nearby region was used to induce a single double-strand break (DSB). This way, DNA repair protein recruitment to a specific DSB can be detected in real-time (Liu et al., 2020; Wang et al., 2019). Two recent studies combined live imaging of repetitive genomic loci using dCas9 with subsequent DNA FISH after cell fixation through image registry (Guan et al., 2017; Takei et al., 2017) (Figure 3C), raising an exciting possibility to observe spatiotemporal dynamics of genomic DNA and proteins at specific genomic locations of interest even when the sequence is non-repetitive. Finally, combining genome labeling with genome manipulation tools, for example, using CRISPR Cas9-based tools to bring distant genomic sites together (Wang et al., 2018a), and to turn on and off Cas9 activities through photoactivation and deactivation to control DSB generation at high spatiotemporal resolution (Liu et al., 2020; Zou et al., 2021), promises to further expand our capability to dissect chromatin transactions underlying genome maintenance and gene expression regulation.

RNA and nascent polypeptide labeling in live cells

mRNA is an essential intermediate to convert the 1D genetic information encoded in DNA to the 3D cellular structure. Cells regulate RNA transcription, splicing, transport, localization, translation, and degradation to ensure protein synthesis at the right time and the right place. Detection and tracking of single mRNAs in live cells became a reality using fluorescent proteins tethered to transcripts or RNA aptamers binding to fluorogenic dyes (Tutucci et al., 2018). MS2 technology, relying on repeated MS2 binding sites (MBS) bound by fluorescently tagged MS2 coat proteins (MCP), is widely used. When a tagged gene is transcribed, the nascent RNAs appear as a bright fluorescent spot, whose fluorescence intensity traces can be used to infer transcriptional and post-transcriptional dynamics (Figure 4).

The GGGGCC repeat expansion in the intron of C9orf72 is the most common genetic cause of familial amyotrophic lateral sclerosis and frontotemporal dementia. Wang et al., established a reporter for C9ORF72 with both introns and exons fluorescently labeled (Wang et al., 2021a). They found that these repetitive RNAs form nuclear RNA granules. More importantly, the repeats induce introns to be exported into the cytoplasm in a circular form, likely to become the template of the non-canonical non-AUG translation that produces toxic dipeptide repeats.

To visualize the translation dynamics of single mRNAs, we and others used a strategy similar to nascent RNA labeling. Repetitive SunTag epitopes placed at the N terminus of target proteins are labeled by fluorescent single-chain antibody (scFv) as soon as they emerge from ribosomes (Wu et al., 2016). The fluorescence intensity of translation sites can be used to monitor translation dynamics in live cells, or even in live embryos (Dufourt et al., 2021). The SunTag system has been employed to study translation initiation in different reading frames and frameshifting on single mRNAs (Boersma et al., 2019; Lyon et al., 2019)

When different *cis*-elements are placed before or after the SunTag motif, their effects on translation dynamics can be studied at the single mRNA level (Figure 4). Hoek et al. inserted a pre-termination codon (PTC) after the SunTag to study nonsense-mediated mRNA decay (Hoek et al., 2019). They found that multiple ribosomes encountering with PTC are required to trigger RNA decay, instead of a single pioneering round of translation as hypothesized previously. Goldman et al. placed strong stalling poly-A sequences before the stop codon and observed massive queues of collided ribosomes before poly-A. The collided ribosomes take much longer to clear from mRNAs than those in normal elongation and termination, explaining how cells differentiate transient pausing and stalling (Goldman et al., 2021).

The SunTag system has also been used to study the translation and replication of viruses. HIV-1 viral RNA serves both as a template for Gag/Gag-Pol translation and as a genome for new viruses. Chen et al. have incorporated SunTag into HIV-1 RNA to visualize its translation (Chen et al., 2020). They found that the viral Gag protein preferentially packages non-translating

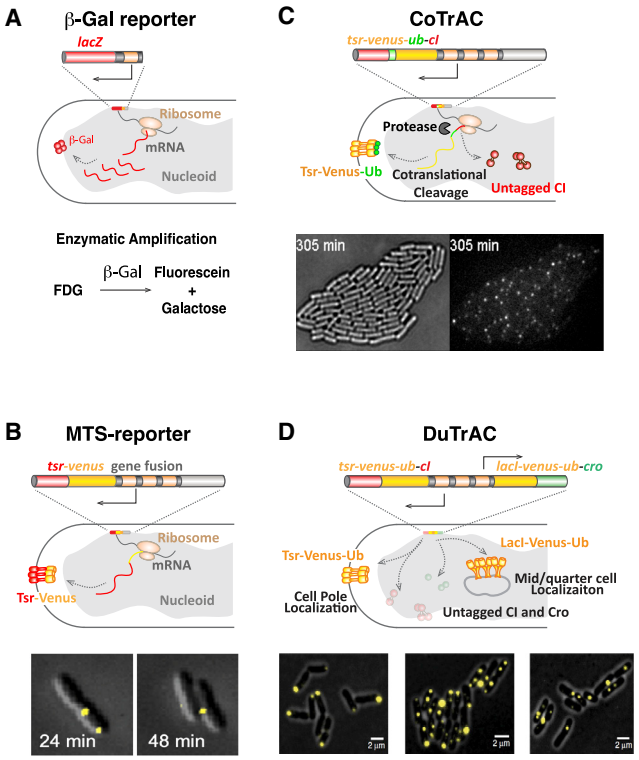

Figure 5. Illustration of real time reporters of single protein molecule expression

(A–D) Real-time detection of expressed single protein molecules by enzymatic amplification using β-Gal as a reporter (A), by confined diffusion using a membrane-targeted single-molecule Tsr-Venus reporter (B), without a tag using the co-translational activation by cleavage (CoTrAC) strategy (C), and in two subcellular localizations using DuTrAC (D).

The bottom is corresponding fluorescence images used to count the number of protein molecules produced in real-time. Source: Fang et al. (2018).

RNAs. To monitor the initial infection stages, Boersma et al. have constructed a replication-competent virus incorporating SunTag at the N terminus (Boersma et al., 2020). They observed single viral infection events and subsequent replication and translation events. They identified that the initial replication step as the major bottleneck for infection and the best opportunity for the host to counteract the virus.

Protein expression labeling

Accurate counting of expressed proteins in real-time is critical for quantitative assessments of protein's biochemical activities in cells. To detect single protein molecules as they are expressed, early work used two concepts: signal enhancement by enzymatic amplification, and single-molecule detection by confinement (Figure 5). In one (Cai et al., 2006), single *E. coli* or yeast cells expressing a chromosomal *lacZ* gene encoding β-galactosidase (β-gal) were trapped individually in enclosed microfluidic chambers (Figure 5A). When a β-gal tetramer is produced, it hydrolyzes fluorogenic substrates included in the growth medium and leads to amplified detectable fluorescence signals in the chamber. In the other (Yu et al., 2006), a fast-maturing yellow fluorescent protein, Venus, is fused to the membrane protein Tsr in *E. coli*. Venus maturation for fluorescence after the expression is the fastest (~5–7 min in live *E. coli* cells) among all available FPs, enabling gene expression dynamic to be probed at high time resolution. Tsr spatially confines Venus molecules on the membrane, slowing down its diffusion for single-molecule detection (Figure 5B). The same concept was later applied to study the dynamics of local translation in neuronal dendrites (Ifrim et al., 2015; Na et al., 2016). Additionally, while not in real-time, single-molecule counting of expressed proteins of low abundance have been made possible by using the protein's natural localization signal (Taniguchi et al., 2010), fixing cells (Lepore et al., 2019), or mechanically confining the diffusion of cytoplasmic proteins (Okumus et al., 2016).

One drawback of these single-molecule gene expression reporters is their fusion to the protein of interest (POI) may disrupt function. To overcome this limitation, a new strategy termed co-translational activation by cleavage (CoTrAC; Figure 5C) was developed (Hensel et al., 2012). In this strategy, the POI is fused to Tsr-Venus, with yeast ubiquitin inserted in between. The yeast ubiquitin C-terminal hydrolase (encoded by ubp1) was coexpressed to cotranslationally cleave the emergent polypeptide after the C-terminal ubiquitin (Ub) residue, allowing the POI to be released from the fused reporter, while its expression is monitored by counting the number of Tsr-Venus-Ub reporter molecules detected on the membrane. This strategy ensures accurate counting of the expressed protein without tagging because, for each POI, exactly one reporter molecule is produced.

More recently, a dual single-molecule gene expression reporting system, termed Dual CoTrAC (DuTrAC; Figure 5D), was developed to monitor the expression dynamics of two proteins simultaneously in the same cell (Fang et al., 2018). In DuTrAC, two different subcellular localization tags, Tsr-Venus (cell pole localization) and LacI-Venus (mid or quarter cell localization due to its binding to a tandem lacO site-containing plasmid), instead of two FPs of different colors, were used. The high localization precision (30–40 nm) of a single Venus molecule in live *E. coli* cells makes it possible to distinguish two reporter molecules based on their subcellular locations and avoids disparity in the maturation rates of FPs. Combined with CoTrAC, the expression dynamics of two mutually regulating TFs of the λ phage, CI and Cro, were faithfully reported (Fang et al., 2018).

Many mammalian proteins localize to specific subcellular locations. The concepts of subcellular single-molecule detection and activation by co-translational cleavage can be further generalized to a third or even fourth reporter of the same color and in mammalian cells.

SINGLE-MOLECULE MANIPULATION

"Perturb and observe" is a universal and powerful strategy to understand the natural world. The ability to manipulate single molecules by applying piconewton forces and record their response with sub-nanometer precision has transformed our understanding of molecular mechanisms of diverse biological processes, ranging from protein folding to cell surface receptor function.

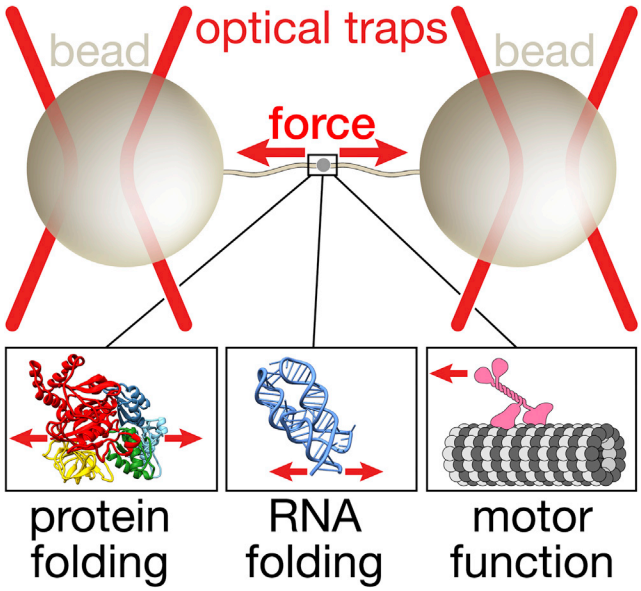

Figure 6. Illustration of an optical tweezers experiment and select biological applications

Mechanical interrogation using optical tweezers

Optical tweezers use light to mechanically manipulate individual molecules. Soon after the technique was invented by Arthur Ashkin some 30 years ago, optical tweezers found widespread use to interrogate biological macromolecules by measuring how they respond to the application of small, precisely defined forces (Killian et al., 2018). The biological importance of mechanical force is intuitively clear for "mechanical" processes that range in scale from the contraction of a muscle to the pulling of condensed chromosomes through the viscous cytosol during mitosis. However, mechanical force is now recognized as a crucial aspect of numerous cellular processes, including membrane fusion, molecular motor function, and the synthesis, folding, and degradation of proteins. The forces associated with these processes typically fall into the piconewton (pN) range, which is readily accessible with optical tweezers. Steady increases in the spatial and temporal resolution of optical tweezers experiments now permit the detection of very small (subnanometer) responses of the system under study on fast (microsecond) timescales. These features make optical tweezers a very attractive and appropriate tool for mechanistic studies of diverse biological systems. Some recent examples and developments are introduced in this section.

Optical tweezers experiments typically require the macromolecule of interest to be tethered to small functionalized beads that are held in the optical traps to serve as force probes (Figure 6). The properties of the trap and the beads are key factors in determining the spatiotemporal resolution and the type of information that can be extracted from the measurements. For example, increasing the stiffness of the optical traps enabled the observation of protein folding at very high time resolution, showing that the actual folding process occurs on the microsecond timescale and validating key theoretical predictions from the energy landscape theory of protein folding (Neupane et al., 2016). Recently, the development of germanium nanospheres greatly increased the spatiotemporal resolution of optical tweezers measurements, revealing previously unresolved features of the microtubule-based kinesin motor protein (Sudhakar et al., 2021). New measurement protocols have also improved the time resolution of optical tweezers measurements, illuminating the inner workings of cardiac myosin (Woody et al., 2019).

Early optical tweezer experiments were limited to long nucleic acids and relatively simple proteins that are easily modified biochemically. Advances in sample preparation have allowed more complex macromolecules to be investigated. For instance, optical tweezers studies have shed light on the kinetics and energetics of membrane fusion driven by the folding and assembly of SNARE proteins (Zhang and Hughson, 2021). The approach also enabled studies of co-transcriptional folding of the signal recognition particle RNA (Fukuda et al., 2020) as well as the roles of the ribosome and molecular chaperones on the folding of nascent proteins (Liu et al., 2019). Together with commercially available high-resolution instruments, simplified sample preparation strategies (Maciuba et al., 2021) further expand the reach of the technique. Advances in instrumentation also enable novel measurement modalities. For instance, a quadruple optical trap can manipulate two DNA molecules independently to measure key steps in DNA DSB repair (Brouwer et al., 2016). The development of an angular optical trap enabled the determination of the torsional stiffness of single and double chromatin fibers, the supercoiled structures during DNA replication (Le et al., 2019). Combining optical tweezers with DNA origami yielded precise measurements of sequence resolved stacking forces in DNA duplexes, fundamentally important for understanding and modeling nucleic acid structure and dynamics (Kilchherr et al., 2016). These advances, combined with single-fluorophore detection (see section Integration of single-molecule fluorescence and force measurements), make optical tweezers an ever more powerful tool for mechanistic studies of biological macromolecules.

Integration of single-molecule fluorescence and force measurements

Most single-molecule experiments measure just a single observable versus time, typically distance in either optical tweezers or fluorescence experiments. For more complex multiple-component systems that better mimic the physiological conditions, this is no longer is sufficient. Combing optical tweezers with single-molecule fluorescence detection, affectionately called "fleezers" for "fluorescence and tweezers," increases the number of measurable biophysical quantities, and–more importantly–provide a way of delivering real-time control to manipulate the system. For example, fleezers have been used to simultaneously measure the conformational state of a helicase via smFRET and DNA unwinding via optical tweezers (Figures 7A and 7B) (Comstock et al., 2015). Fleezers experiments also reveal conformational changes occurring in response to physiological levels of mechanical force (Hohng et al., 2007), and led to novel functional insights, for example, how DNA sequence and methylation modulate mechanical stability of a nucleosome (Ngo et al., 2015) and how Cas9's binding to off-target DNA is greatly escalated with increasing tension on DNA (Newton et al., 2019). In a tour de force experiment, mechanical unfolding

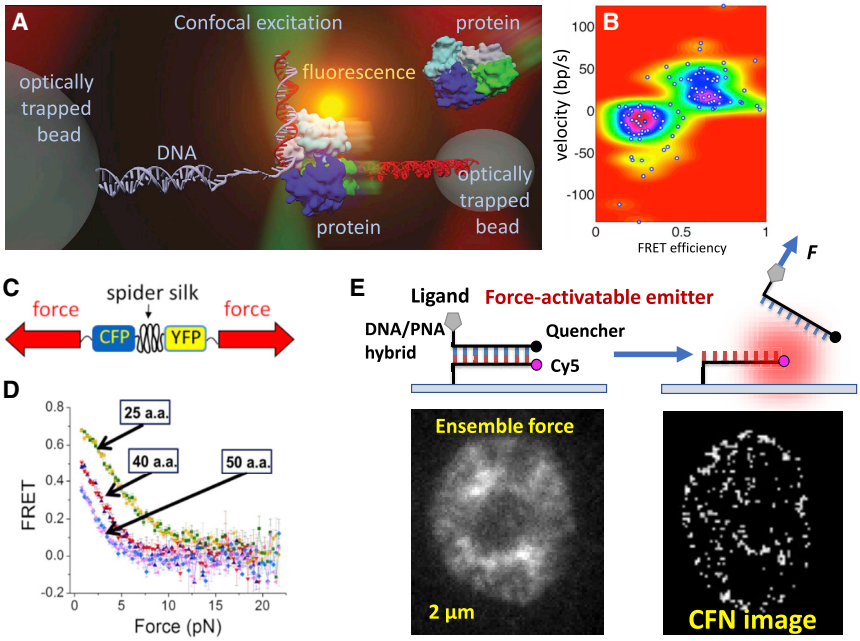

Figure 7. Illustration of fleezers and tension gauge tether technologies and their applications

(A and B) Ultrahigh-resolution optical tweezers with single-fluorophore sensitivity. In (A), dual optical traps apply forces to DNA segments connecting optically trapped beads and detect DNA length changes induced by the enzymatic activity of DNA unzipping by a protein at ~0.1-nm resolution. At the same time, confocal fluorescence excitation and detection can measure the protein's structural changes. Source: Matthew Comstock. in (B) one sees the correlation between DNA unzipping activity, measured by optical tweezers and expressed in reaction velocity, and protein structural changes, measured by FRET. Source: Comstock et al. (2015).

(C) Schematics of FRET-based tension sensor. FRET donor (CFP) and acceptor (YFP) are separated by a spider silk peptide, which serves as a linear spring. When force is applied across the sensor, FRET decrease due to the stretching of the peptide.

(D) Fleezers calibration of tension sensor of a different number of amino acids comprising the spider silk-derived spring element. Note that the shortest peptide (25 a.a.) has the largest range of FRET signal and is sensitive to the largest force range. Source: Brenner et al. (2016).

(E) Schematics of cellular force nanoscopy (CFN). Using quenched TGT, fluorophores activated by force-induced TGT rupture are localized one at a time.

(F) Ensemble (left) and super-resolution force imaging (right). Source: Zhao et al. (2020).

and refolding of a green fluorescence protein was detected via fluorescence signal disappearance and appearance, respectively (Ganim and Rief, 2017). Interestingly, fluorescence disappeared 3.5 ms before abrupt unfolding whereas no intermediate fluorescence state delay was observed during refolding.

Optical tweezers suffer from low throughput, particularly exacerbated when combined with fluorescence due to incomplete labeling and photobleaching. Although commercial implementation alleviates the difficulty, optical tweezers still apply force to one molecule at a time. One way to increase throughput is to bypass optical tweezers altogether and apply force using rigid DNA origami structures. Constant forces, adjustable by designing different origami structures, can be applied to hundreds of molecules and their force-dependent conformational dynamics read out in parallel (Nickels et al., 2016). The effective force applied is calibrated using the force-dependence of conformational dynamics of DNA four-way (Holliday) junctions, which had been previously determined using fleezers (Hohng et al., 2007). Magnetic tweezers can also apply forces coincident with fluorescence detection and probe dozens of molecules simultaneously, potentially improving the throughput. An added bonus is that magnetic tweezers can induce supercoiling in torsionally constrained DNA. For example, a magnetic fleezers study revealed sequence dependence of torsion-driven transitions between B and Z forms of DNA (Kim et al., 2021). Yet another method to apply force during high-resolution single-molecule measurements is nanopore tweezers. For example, the directional translocation of a helicase along a single-stranded DNA was detected by changes in electric current through a nanopore at sub-nucleotide and sub-ms resolution, showing, surprisingly, that the speed of movement is DNA sequence-dependent (Craig et al., 2017). As electrical current through a single ion channel has been detected together with smFRET to analyze ion channel conformation (Sasmal and Lu, 2014), we anticipate that nanopore fleezers will soon become a reality.

Single-molecule force sensors for live-cell mechanical measurement

It is now widely appreciated that cancer cells and stem cells can change their cell fate (differentiation, metastasis, etc.) in response to mechanical cues. They use mechano-sensitive membrane receptors to sense their mechanical environment. In order to understand how molecular level mechanics trigger cellular responses, we need tools to examine the forces applied across individual proteins in living cells. For example, FRET-based tension sensors exploit a spider silk peptide flanked by a CFP and YFP as a tension sensing element. The tension sensor was calibrated using fleezers (Grashoff et al., 2010; Hohng et al., 2007) (Brenner et al., 2016) (Figures 7C and 7D) (see section titled Integeration of single-molecule fluorescence and force measurements). This approach was extended by adopting proteins that denature at a defined force as the tension sensing element (Austen et al., 2015). These sensors were used to detect forces applied by single integrin molecules through smFRET measurements (Tan et al., 2020).

To define the single molecular forces required to activate signaling through a ligand-receptor bond, the tension gauge tether (TGT) approach was developed. In TGT, a ligand is immobilized to a surface through a rupturable tether (Wang and Ha, 2013). If the tether is stronger than the force needed to activate signaling through the receptor, mechanical signaling occurs. Otherwise, the tethers rupture and there is no signaling. Using a range of

tethers with tunable tension tolerance, it was shown that mammalian cells apply a peak tension of about 40 pN to single integrin-ligand bonds during initial adhesion (Wang and Ha, 2013) and that Notch activation requires forces between 4 and 12 pN (Chowdhury et al., 2016). Another advantage of TGT is that it can record the history of single-molecule forces. By fluorescent labeling of the ligand-conjugated strand (top strand), fluorescence is lost upon TGT rupture. By conjugating a fluorophore to the bottom strand and a quencher to the top strand, there is no fluorescence until TGT rupture (Figure 7E), and single-fluorophore signals appear over time, which can be localized to map single-molecule forces at super-resolution (Figure 7F) (Zhao et al., 2020).

The irreversible TGT rupture is particularly advantageous for obtaining a cumulative recording of mechanical events for many cells in parallel. However, some applications may benefit from a reversible readout. In this case, continuous real-time imaging is required for measuring the force. Reversible fluorescence-based tension sensors can be constructed using DNA hairpins (Blakely et al., 2014; Zhang et al., 2014). One limitation of this approach is that DNA hairpins open at low forces (4–15 pN depending on the stem length and sequence) and cannot differentiate forces between 20 and 50 pN, a range critical for integrins. Recently, a hybrid approach combining the reversible nature of hairpin-based sensors and the high force range of TGT was demonstrated (Li et al., 2021).

The tension tolerance of TGT should depend on the loading rate, a measure of how quickly the force rises because a bond always ruptures at a given mechanical force as long as one is willing to wait. It should be straightforward to measure TGT rupture force at different loading rates (Chowdhury et al., 2016), but the physiological level of loading rate for a given receptor-ligand pair also needs to be determined before TGTs can be accurately calibrated.

CONCLUSION

In this review, we discussed recent advances in some of the most popular categories of single-molecule technologies. These established technologies have now been widely used in diverse fields ranging from phage biology and microbiology to neurobiology, immunology, and cancer biology, making contributions to fundamental biomedical and clinical research. In recognition of the transformative force, single-molecule technologies have brought to biological sciences, two recent Nobel prizes were awarded for super-resolution and single-molecule fluorescence microscopy (2014, Chemistry, shared by Moerner, Hell and Betzig) and optical tweezers (2018, Physics, Ashkin). Yet, cutting-edge single-molecule technologies are still limited to highly specialized laboratories because of their complex and lab-specific instrumentation, stringent sample and reagents preparation, and tailored data analysis. These requirements impose a substantial barrier for non-specialized laboratories in the larger biomedical research community to adopt and benefit from these impactful technologies. Moving forward, we anticipate that commercialization, the establishment of regional and national single-molecule technology centers, and online and in-person training will lead to the democratization of single-molecule technologies so that biologists can apply these tools in their laboratories without having to collaborate with specialists.

DECLARATION OF INTERESTS

S.M. is a member of the Editorial Board of Molecular Cell. T.H. is an immediate family member of an individual on the Editorial Board of Molecular Cell.

REFERENCES

Arslan, S., Khafizov, R., Thomas, C.D., Chemla, Y.R., and Ha, T. (2015). Protein structure. Engineering of a superhelicase through conformational control. Science *348*, 344–347.

Asher, W.B., Geggier, P., Holsey, M.D., Gilmore, G.T., Pati, A.K., Meszaros, J., Terry, D.S., Mathiasen, S., Kaliszewski, M.J., McCauley, M.D., et al. (2021). Single-molecule FRET imaging of GPCR dimers in living cells. Nat. Methods *18*, 397–405.

Austen, K., Ringer, P., Mehlich, A., Chrostek-Grashoff, A., Kluger, C., Klingner, C., Sabass, B., Zent, R., Rief, M., and Grashoff, C. (2015). Extracellular rigidity sensing by talin isoform-specific mechanical linkages. Nat. Cell Biol. *17*, 1597–1606.

Ávalos Prado, P., Häfner, S., Comoglio, Y., Wdziekonski, B., Duranton, C., Attali, B., Barhanin, J., and Sandoz, G. (2021). KCNE1 is an auxiliary subunit of two distinct ion channel superfamilies. Cell *184*, 534–544, e11.

Bintu, B., Mateo, L.J., Su, J.H., Sinnott-Armstrong, N.A., Parker, M., Kinrot, S., Yamaya, K., Boettiger, A.N., and Zhuang, X. (2018). Super-resolution chromatin tracing reveals domains and cooperative interactions in single cells. Science *362*, eaau1783.

Blakely, B.L., Dumelin, C.E., Trappmann, B., McGregor, L.M., Choi, C.K., Anthony, P.C., Duesterberg, V.K., Baker, B.M., Block, S.M., Liu, D.R., and Chen, C.S. (2014). A DNA-based molecular probe for optically reporting cellular traction forces. Nat. Methods *11*, 1229–1232.

Boersma, S., Khuperkar, D., Verhagen, B.M.P., Sonneveld, S., Grimm, J.B., Lavis, L.D., and Tanenbaum, M.E. (2019). Multi-color single-molecule imaging uncovers extensive heterogeneity in mRNA decoding. Cell *178*, 458–472, e19.

Boersma, S., Rabouw, H.H., Bruurs, L.J.M., Pavlovič, T., van Vliet, A.L.W., Beumer, J., Clevers, H., van Kuppeveld, F.J.M., and Tanenbaum, M.E. (2020). Translation and replication dynamics of single RNA viruses. Cell *183*, 1930–1945, e23.

Bohrer, C.H., and Xiao, J. (2020). Complex diffusion in bacteria. Adv. Exp. Med. Biol. *1267*, 15–43.

Brenner, M.D., Zhou, R., Conway, D.E., Lanzano, L., Gratton, E., Schwartz, M.A., and Ha, T. (2016). Spider silk peptide is a compact, linear nanospring ideal for intracellular tension sensing. Nano Lett *16*, 2096–2102.

Brouwer, I., Sitters, G., Candelli, A., Heerema, S.J., Heller, I., de Melo, A.J., Zhang, H., Normanno, D., Modesti, M., Peterman, E.J., and Wuite, G.J.L. (2016). Sliding sleeves of XRCC4-XLF bridge DNA and connect fragments of broken DNA. Nature *535*, 566–569.

Brown, J.M., Roberts, N.A., Graham, B., Waithe, D., Lagerholm, C., Telenius, J.M., De Ornellas, S., Oudelaar, A.M., Scott, C., Szczerbal, I., et al. (2018). A tissue-specific self-interacting chromatin domain forms independently of enhancer-promoter interactions. Nat. Commun. *9*, 3849.

Cai, L., Friedman, N., and Xie, X.S. (2006). Stochastic protein expression in individual cells at the single molecule level. Nature *440*, 358–362.

Chen, J., Liu, Y., Wu, B., Nikolaitchik, O.A., Mohan, P.R., Chen, J., Pathak, V.K., and Hu, W.-S. (2020). Visualizing the translation and packaging of HIV-1 full-length RNA. Proc. Natl. Acad. Sci. USA *117*, 6145–6155.

Chen, Z., Cao, Y., Lin, C.-W., Alvarez, S., Oh, D., Yang, P., and Groves, J.T. (2021). Nanopore-mediated protein delivery enabling three-color single-molecule tracking in living cells. Proc. Natl. Acad. Sci. USA *118*, e2012229118.

Chowdhury, F., Li, I.T., Ngo, T.T., Leslie, B.J., Kim, B.C., Sokoloski, J.E., Weiland, E., Wang, X., Chemla, Y.R., Lohman, T.M., and Ha, T. (2016). Defining single molecular forces required for notch activation using Nano yoyo. Nano Lett *16*, 3892–3897.

Comstock, M.J., Whitley, K.D., Jia, H., Sokoloski, J., Lohman, T.M., Ha, T., and Chemla, Y.R. (2015). Protein structure. Direct observation of structure-function relationship in a nucleic acid-processing enzyme. Science *348*, 352–354.

Coulon, A., Ferguson, M.L., de Turris, V., Palangat, M., Chow, C.C., and Larson, D.R. (2014). Kinetic competition during the transcription cycle results in stochastic RNA processing. Elife *3*, e03939.

Craig, J.M., Laszlo, A.H., Brinkerhoff, H., Derrington, I.M., Noakes, M.T., Nova, I.C., Tickman, B.I., Doering, K., de Leeuw, N.F., and Gundlach, J.H. (2017). Revealing dynamics of helicase translocation on single-stranded DNA using high-resolution nanopore tweezers. Proc. Natl. Acad. Sci. USA *114*, 11932–11937.

Deng, W., Shi, X., Tjian, R., Lionnet, T., and Singer, R.H. (2015). CASFISH: CRISPR/Cas9-mediated in situ labeling of genomic loci in fixed cells. Proc. Natl. Acad. Sci. USA *112*, 11870–11875.

Dickinson, D.J., Schwager, F., Pintard, L., Gotta, M., and Goldstein, B. (2017). A single-cell biochemistry approach reveals PAR complex dynamics during cell polarization. Dev. Cell *42*, 416–434, e11.

Dufourt, J., Bellec, M., Trullo, A., Dejean, M., De Rossi, S., Favard, C., and Lagha, M. (2021). Imaging translation dynamics in live embryos reveals spatial heterogeneities. Science *372*, 840–844.

Elf, J., and Barkefors, I. (2019). Single-molecule kinetics in living cells. Annu. Rev. Biochem. *88*, 635–659.

Fang, X., Liu, Q., Bohrer, C., Hensel, Z., Han, W., Wang, J., and Xiao, J. (2018). Cell fate potentials and switching kinetics uncovered in a classic bistable genetic switch. Nat. Commun. *9*, 2787.

Fukuda, S., Yan, S., Komi, Y., Sun, M., Gabizon, R., and Bustamante, C. (2020). The biogenesis of SRP RNA is modulated by an RNA folding intermediate attained during transcription. Mol. Cell *77*, 241–250, e8.

Ganim, Z., and Rief, M. (2017). Mechanically switching single-molecule fluorescence of GFP by unfolding and refolding. Proc. Natl. Acad. Sci. USA *114*, 11052–11056.

Gebhardt, J.C., Suter, D.M., Roy, R., Zhao, Z.W., Chapman, A.R., Basu, S., Maniatis, T., and Xie, X.S. (2013). Single-molecule imaging of transcription factor binding to DNA in live mammalian cells. Nat. Methods *10*, 421–426.

Goldman, D.H., Livingston, N.M., Movsik, J., Wu, B., and Green, R. (2021). Live-cell imaging reveals kinetic determinants of quality control triggered by ribosome stalling. Mol. Cell *81*, 1830–1840, e8.

Grashoff, C., Hoffman, B.D., Brenner, M.D., Zhou, R., Parsons, M., Yang, M.T., McLean, M.A., Sligar, S.G., Chen, C.S., Ha, T., and Schwartz, M.A. (2010). Measuring mechanical tension across vinculin reveals regulation of focal adhesion dynamics. Nature *466*, 263–266.

Grimm, J.B., English, B.P., Choi, H., Muthusamy, A.K., Mehl, B.P., Dong, P., Brown, T.A., Lippincott-Schwartz, J., Liu, Z., Lionnet, T., and Luke, L.D. (2016). Bright photoactivatable fluorophores for single-molecule imaging. Nat. Methods *13*, 985–988.

Guan, J., Liu, H., Shi, X., Feng, S., and Huang, B. (2017). Tracking multiple genomic elements using correlative CRISPR imaging and sequential DNA FISH. Biophys. J. *112*, 1077–1084.

Ha, T., Enderle, T., Ogletree, D.F., Chemla, D.S., Selvin, P.R., and Weiss, S. (1996). Probing the interaction between two single molecules: fluorescence resonance energy transfer between a single donor and a single acceptor. Proc. Natl. Acad. Sci. USA *93*, 6264–6268.

Hensel, Z., Feng, H., Han, B., Hatem, C., Wang, J., and Xiao, J. (2012). Stochastic expression dynamics of a transcription factor revealed by single-molecule noise analysis. Nat. Struct. Mol. Biol. *19*, 797–802.

Hoek, T.A., Khuperkar, D., Lindeboom, R.G.H., Sonneveld, S., Verhagen, B.M.P., Boersma, S., Vermeulen, M., and Tanenbaum, M.E. (2019). Single-molecule imaging uncovers rules governing nonsense-mediated mRNA decay. Mol. Cell *75*, 324–339, e11.

Hohng, S., Joo, C., and Ha, T. (2004). Single-molecule three-color FRET. Biophys. J. *87*, 1328–1337.

Hohng, S., Zhou, R., Nahas, M.K., Yu, J., Schulten, K., Lilley, D.M., and Ha, T. (2007). Fluorescence-force spectroscopy maps two-dimensional reaction landscape of the holliday junction. Science *318*, 279–283.

Hou, S., Exell, J., and Welsher, K. (2020). Real-time 3D single molecule tracking. Nat. Commun. *11*, 3607.

Hwang, H., Kim, H., and Myong, S. (2011). Protein induced fluorescence enhancement as a single molecule assay with short distance sensitivity. Proc. Natl. Acad. Sci. USA *108*, 7414–7418.

Ifrim, M.F., Williams, K.R., and Bassell, G.J. (2015). Single-molecule imaging of PSD-95 mRNA translation in dendrites and its dysregulation in a mouse model of fragile X syndrome. J. Neurosci. *35*, 7116–7130.

Jain, A., Liu, R., Ramani, B., Arauz, E., Ishitsuka, Y., Ragunathan, K., Park, J., Chen, J., Xiang, Y.K., and Ha, T. (2011). Probing cellular protein complexes using single-molecule pull-down. Nature *473*, 484–488.

Kapanidis, A.N., Lee, N.K., Laurence, T.A., Doose, S., Margeat, E., and Weiss, S. (2004). Fluorescence-aided molecule sorting: analysis of structure and interactions by alternating-laser excitation of single molecules. Proc. Natl. Acad. Sci. USA *101*, 8936–8941.

Khaw, I., Croop, B., Tang, J., Möhl, A., Fuchs, U., and Han, K.Y. (2018). Flat-field illumination for quantitative fluorescence imaging. Opt. Express *26*, 15276–15288.

Kilchherr, F., Wachauf, C., Pelz, B., Rief, M., Zacharias, M., and Dietz, H. (2016). Single-molecule dissection of stacking forces in DNA. Science *353*, aaf5508.

Killian, J.L., Ye, F., and Wang, M.D. (2018). Optical tweezers: a force to be reckoned with. Cell *175*, 1445–1448.

Kim, S.H., Jung, H.J., Lee, I.-B., Lee, N.-K., and Hong, S.-C. (2021). Sequence-dependent cost for Z-form shapes the torsion-driven B-Z transition via close interplay of Z-DNA and DNA bubble. Nucleic Acids Res *49*, 3651–3660.

König, I., Zarrine-Afsar, A., Aznauryan, M., Soranno, A., Wunderlich, B., Dingfelder, F., Stüber, J.C., Plückthun, A., Nettels, D., and Schuler, B. (2015). Single-molecule spectroscopy of protein conformational dynamics in live eukaryotic cells. Nat. Methods *12*, 773–779.

Lavis, L.D. (2017). Teaching old dyes new tricks: biological probes built from fluoresceins and rhodamines. Annu. Rev. Biochem. *86*, 825–843.

Le, T.T., Gao, X., Park, S.H., Lee, J., Inman, J.T., Lee, J.H., Killian, J.L., Badman, R.P., Berger, J.M., and Wang, M.D. (2019). Synergistic coordination of chromatin torsional mechanics and topoisomerase activity. Cell *179*, 619–631, e15.

Lepore, A., Taylor, H., Landgraf, D., Okumus, B., Jaramillo-Riveri, S., McLaren, L., Bakshi, S., Paulsson, J., and Karoui, M.E. (2019). Quantification of very low-abundant proteins in bacteria using the HaloTag and epi-fluorescence microscopy. Sci. Rep. *9*, 7902.

Lerner, E., Barth, A., Hendrix, J., Ambrose, B., Birkedal, V., Blanchard, S.C., Börner, R., Sung Chung, H., Cordes, T., Craggs, T.D., et al. (2021). FRET-based dynamic structural biology: challenges, perspectives and an appeal for open-science practices. Elife *10*, e60416.

Li, H., Zhang, C., Hu, Y., Liu, P., Sun, F., Chen, W., Zhang, X., Ma, J., Wang, W., Wang, L., et al. (2021). A reversible shearing DNA probe for visualizing mechanically strong receptors in living cells. Nat Cell Biol. *23*, 642–651.

Liauw, B.W.-H., Afsari, H.S., and Vafabakhsh, R. (2021). Conformational rearrangement during activation of a metabotropic glutamate receptor. Nat. Chem. Biol. *17*, 291–297.

Liu, K., Maciuba, K., and Kaiser, C.M. (2019). The ribosome cooperates with a chaperone to guide multi-domain protein folding. Mol. Cell *74*, 310–319, e7.

Liu, Y., Zou, R.S., He, S., Nihongaki, Y., Li, X., Razavi, S., Wu, B., and Ha, T. (2020). Very fast CRISPR on demand. Science *368*, 1265–1269.

Lyon, K., Aguilera, L.U., Morisaki, T., Munsky, B., and Stasevich, T.J. (2019). Live-cell single RNA imaging reveals bursts of translational frameshifting. Mol. Cell *75*, 172–183, e9.

Maciuba, K., Zhang, F., and Kaiser, C.M. (2021). Facile tethering of stable and unstable proteins for optical tweezers experiments. Biophys. J. *120*, 2691–2700.

Mao, C.-P., Wang, S.-C., Su, Y.-P., Tseng, S.-H., He, L., Wu, A.A., Roden, R.B.S., Xiao, J., and Hung, C.-F. (2021). Protein detection in blood with single-molecule imaging. Sci. Adv. *7*, eabg6522.

Na, Y., Park, S., Lee, C., Kim, D.-K., Park, J.M., Sockanathan, S., Huganir, R.L., and Worley, P.F. (2016). Real-time imaging reveals properties of glutamate-induced arc/Arg 3.1 translation in neuronal dendrites. Neuron *91*, 561–573.

Neupane, K., Foster, D.A., Dee, D.R., Yu, H., Wang, F., and Woodside, M.T. (2016). Direct observation of transition paths during the folding of proteins and nucleic acids. Science *352*, 239–242.

Newton, M.D., Taylor, B.J., Driessen, R.P.C., Roos, L., Cvetesic, N., Allyjaun, S., Lenhard, B., Cuomo, M.E., and Rueda, D.S. (2019). DNA stretching induces Cas9 off-target activity. Nat. Struct. Mol. Biol. *26*, 185–192.

Ngo, T.T., Zhang, Q., Zhou, R., Yodh, J.G., and Ha, T. (2015). Asymmetric unwrapping of nucleosomes under tension directed by DNA local flexibility. Cell *160*, 1135–1144.

Nickels, P.C., Wünsch, B., Holzmeister, P., Bae, W., Kneer, L.M., Grohmann, D., Tinnefeld, P., and Liedl, T. (2016). Molecular force spectroscopy with a DNA origami-based nanoscopic force clamp. Science *354*, 305–307.

Okumus, B., Landgraf, D., Lai, G.C., Bakshi, S., Arias-Castro, J.C., Yildiz, S., Huh, D., Fernandez-Lopez, R., Peterson, C.N., Toprak, E., et al. (2016). Mechanical slowing-down of cytoplasmic diffusion allows in vivo counting of proteins in individual cells. Nat. Commun. *7*, 11641.

Ovesný, M., Křížek, P., Borkovec, J., Svindrych, Z., and Hagen, G.M. (2014). ThunderSTORM: a comprehensive ImageJ plug-in for PALM and STORM data analysis and super-resolution imaging. Bioinformatics *30*, 2389–2390.

Park, K.-H., Kim, S., Lee, S.-J., Cho, J.-E., Patil, V.V., Dumbrepatil, A.B., Song, H.-N., Ahn, W.-C., Joo, C., Lee, S.-G., et al. (2020). Tetrameric architecture of an active phenol-bound form of the AAA(+) transcriptional regulator DmpR. Nat. Commun. *11*, 2728.

Persson, F., Lindén, M., Unoson, C., and Elf, J. (2013). Extracting intracellular diffusive states and transition rates from single-molecule tracking data. Nat. Methods *10*, 265–269.

Qiu, Y., Antony, E., Doganay, S., Koh, H.R., Lohman, T.M., and Myong, S. (2013). Srs2 prevents Rad51 filament formation by repetitive motion on DNA. Nat. Commun. *4*, 2281.

Redding, S., Sternberg, S.H., Marshall, M., Gibb, B., Bhat, P., Guegler, C.K., Wiedenheft, B., Doudna, J.A., and Greene, E.C. (2015). Surveillance and processing of foreign DNA by the Escherichia coli CRISPR-Cas system. Cell *163*, 854–865.

Sasmal, D.K., and Lu, H.P. (2014). Single-molecule patch-clamp FRET microscopy studies of NMDA receptor ion channel dynamics in living cells: revealing the multiple conformational states associated with a channel at its electrical off state. J. Am. Chem. Soc. *136*, 12998–13005.

Schmidt, R., Weihs, T., Wurm, C.A., Jansen, I., Rehman, J., Sahl, S.J., and Hell, S.W. (2021). MINFLUX nanometer-scale 3D imaging and microsecond-range tracking on a common fluorescence microscope. Nat. Commun. *12*, 1478.

Sudhakar, S., Abdosamadi, M.K., Jachowski, T.J., Bugiel, M., Jannasch, A., and Schäffer, E. (2021). Germanium nanospheres for ultraresolution picotensiometry of kinesin motors. Science *371*, eabd9944.

Sungkaworn, T., Jobin, M.-L., Burnecki, K., Weron, A., Lohse, M.J., and Calebiro, D. (2017). Single-molecule imaging reveals receptor-G protein interactions at cell surface hot spots. Nature *550*, 543–547.

Takei, Y., Shah, S., Harvey, S., Qi, L.S., and Cai, L. (2017). Multiplexed dynamic imaging of genomic loci by combined CRISPR imaging and DNA sequential FISH. Biophys. J. *112*, 1773–1776.

Tan, S.J., Chang, A.C., Anderson, S.M., Miller, C.M., Prahl, L.S., Odde, D.J., and Dunn, A.R. (2020). Regulation and dynamics of force transmission at individual cell-matrix adhesion bonds. Sci. Adv. *6*, eaax0317.

Taniguchi, Y., Choi, P.J., Li, G.-W., Chen, H., Babu, M., Hearn, J., Emili, A., and Xie, X.S. (2010). Quantifying E. coli proteome and transcriptome with single-molecule sensitivity in single cells. Science *329*, 533–538.

Tokunaga, M., Imamoto, N., and Sakata-Sogawa, K. (2008). Highly inclined thin illumination enables clear single-molecule imaging in cells. Nat. Methods *5*, 159–161.

Tutucci, E., Livingston, N.M., Singer, R.H., and Wu, B. (2018). Imaging mRNA in vivo, from birth to death. Annu. Rev. Biophys. *47*, 85–106.

Wan, Y., Anastasakis, D.G., Rodriguez, J., Palangat, M., Gudla, P., Zaki, G., Tandon, M., Pegoraro, G., Chow, C.C., Hafner, M., and Larson, D.R. (2021). Dynamic imaging of nascent RNA reveals general principles of transcription dynamics and stochastic splice site selection. Cell *184*, 2878–2895, e20.

Wang, H., Nakamura, M., Abbott, T.R., Zhao, D., Luo, K., Yu, C., Nguyen, C.M., Lo, A., Daley, T.P., La Russa, M., et al. (2019). CRISPR-mediated live imaging of genome editing and transcription. Science *365*, 1301–1305.

Wang, H., Xu, X., Nguyen, C.M., Liu, Y., Gao, Y., Lin, X., Daley, T., Kipniss, N.H., La Russa, M., and Qi, L.S. (2018a). CRISPR-mediated programmable 3D genome positioning and nuclear organization. Cell *175*, 1405–1417, e14.

Wang, S., Latallo, M.J., Zhang, Z., Huang, B., Bobrovnikov, D.G., Dong, D., Livingston, N.M., Tjoeng, W., Hayes, L.R., Rothstein, J.D., et al. (2021a). Nuclear export and translation of circular repeat-containing intronic RNA in C9ORF72-ALS/FTD. Nat. Commun. *12*, 4908.

Wang, X., and Ha, T. (2013). Defining single molecular forces required to activate integrin and notch signaling. Science *340*, 991–994.

Wang, X., Park, S., Zeng, L., Jain, A., and Ha, T. (2018b). Toward single-cell single-molecule pull-down. Biophys. J. *115*, 283–288.

Wang, Y., Cottle, W.T., Wang, H., Feng, X.A., Mallon, J., Gavrilov, M., Bailey, S., and Ha, T. (2021b). Genome oligopaint via local denaturation fluorescence in situ hybridization. Mol. Cell *81*, 1566–1577, e8.

Wilson, H., and Wang, Q. (2021). ABEL-FRET: tether-free single-molecule FRET with hydrodynamic profiling. Nat. Methods *18*, 816–820.

Woody, M.S., Winkelmann, D.A., Capitanio, M., Ostap, E.M., and Goldman, Y.E. (2019). Single molecule mechanics resolves the earliest events in force generation by cardiac myosin. Elife *8*, e49266.

Wu, B., Eliscovich, C., Yoon, Y.J., and Singer, R.H. (2016). Translation dynamics of single mRNAs in live cells and neurons. Science *352*, 1430–1435.

Xu, J., Qin, G., Luo, F., Wang, L., Zhao, R., Li, N., Yuan, J., and Fang, X. (2019). Automated stoichiometry analysis of single-molecule fluorescence imaging traces via deep learning. J. Am. Chem. Soc. *141*, 6976–6985.

Yang, X., McQuillen, R., Lyu, Z., Phillips-Mason, P., De La Cruz, A., McCausland, J.W., Liang, H., DeMeester, K.E., Santiago, C.C., Grimes, C.L., et al. (2021). A two-track model for the spatiotemporal coordination of bacterial septal cell wall synthesis revealed by single-molecule imaging of FtsW. Nat. Microbiol. *6*, 584–593.

Yu, J., Rao, P., Clark, S., Mitra, J., Ha, T., and Gouaux, E. (2021). Hippocampal AMPA receptor assemblies and mechanism of allosteric inhibition. Nature *594*, 448–453.

Yu, J., Xiao, J., Ren, X., Lao, K., and Xie, X.S. (2006). Probing gene expression in live cells, one protein molecule at a time. Science *311*, 1600–1603.

Zhang, Y., Ge, C., Zhu, C., and Salaita, K. (2014). DNA-based digital tension probes reveal integrin forces during early cell adhesion. Nat. Commun. *5*, 5167.

Zhang, Y., and Hughson, F.M. (2021). Chaperoning SNARE folding and assembly. Annu. Rev. Biochem. *90*, 581–603.

Zhao, Y., Pal, K., Tu, Y., and Wang, X. (2020). Cellular force nanoscopy with 50-nm resolution based on integrin molecular tension imaging and localization. J. Am. Chem. Soc. *142*, 6930–6934.

Zou, R.S., Liu, Y., Wu, B., and Ha, T. (2021). Cas9 deactivation with photocleavable guide RNAs. Mol. Cell *81*, 1553–1565, e8.